Turbo Trellis Coded Hierarchical Modulation for Cooperative Communications

Hua Sun, Yiru Shen, Soon Xin Ng and Lajos Hanzo
School of Electronics and Computer Science, University of Southampton, SO17 1BJ, United Kingdom.
Tel: +44-23-8059 3125, Fax: +44-23-8059 4508
Email: {hs4g09,ys1g10,sxn,lh}@ecs.soton.ac.uk, http://www-mobile.ecs.soton.ac.uk

***Abstract*— A cooperative communication system assisted by Turbo Trellis-Coded Modulation (TTCM) relying on Hierarchical Modulation (HM) is proposed, which invokes iterative soft decoding. Our results demonstrated that the performance of the single-relay aided cooperative system can be improved by at least 4 dB at a BER of 10^{-5}.**

***Index Terms*— Hierarchical modulation, Cooperative communication, TTCM, Soft decoding**

I. Introduction

The existing wireless networks support in excess of 4 billion subscribers, hence it would be impossible to replace all the personal devices or base stations for upgrading the services. Furthermore, maintaining the Quality of Service (QoS) for all subscribers, while aiming for an increased QoS for the upgraded new services would require strict backward compatibility [1], [2]. Hierarchical Modulation (HM), which is also often referred to as layered modulation may be considered as an efficient solution to the above-mentioned upgrading problems. The benefit of HM is that it is capable of manipulating multiple simultaneous data streams by modulating them on to a number of different layers, while the information in the different layers may be demodulated separately [1]. In this way, the upgraded new services may be merged with the already available services, where the original devices may simply switch to a higher number of modulation levels or to a higher coding rate in the upgraded broadcast devices [3].

The HM scheme is well investigated by Alouini in [4], [5] in terms of the general mapping model, the complexity analysis and the BER performance. HM scheme has also been incorporated in cooperative communication systems by C. Hausl [6] and Z. Y. Li [7]. It is showed that by employing HM scheme, the destination node could only demap part of the received signal from the source, while the relay node could provide the rest of the information to assist the entire transmission. Their results illustrated that the performance of the system could be improved without enlarging the complexity of the entire system. In this paper,

1) We proposed a newly designed HM scheme for cooperative communications when communicating over Rayleigh fading channels.
2) A novel Turbo Trellis-Coded HM (TTCHM) scheme was conceived for improving the performance of the entire system.

Our assumption is that the Destination Node (DN) is only capable of receiving 4QAM signals from the Source Node (SN) due to the hostile nature of the fading channel. By contrast, our simulation results demonstrated that with the aid of our TTCHM scheme relying on a single relay, it is possible for the SN to transmit 16QAM or even 64QAM symbols, while maintaining an acceptable BER performance at the DN.

The organization of this paper is as follows. Section II illustrates the system model and the paper's rationale. Section III presents the HM's layering method, while Section IV details the system's block diagram and our communications protocol. Our simulation results and analysis are provided in Section V, while our conclusions are offered in Section VI.

II. System Model

In this section we introduce our TTCHM assisted Decode-And-Forward (DAF) based cooperative communication scheme of Fig. 1. During the first communication Time Slot (TS), the SN would transmit a frame of TTCHM symbols $\{x_1\}$ to both the Relay Node (RN) and DN. Then the RN decodes the stream $\{x_1\}$ to produce the frame $\{x_2\}$, which would be forwarded to the DN during the second TS. The DN would recover the frame $\{x_1\}$ based on the pair of frames received from the SN and RN.

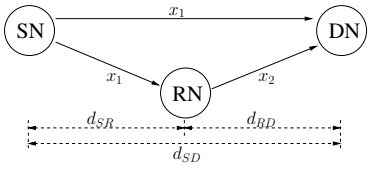

Fig. 1. The model of a single-relay cooperative system.

The financial support of the EPSRC UK under the auspices of the China-UK Science Bridge, the India-UK Advanced Technology Centre and that of the European Union's Seventh Framework Programme (FP7/2007-2013) under the auspices of the CONCERTO project (grant agreement no 288502) is greatly appreciated.

978-1-4673-5939-9/13/$31.00 ©2013 IEEE

We considered an uncorrelated Rayleigh flat-fading channel and the receivers were assumed to acquire perfect Channel State Information (CSI). After the first TS, the symbol received by the DN may be expressed as:

$$y_{SD} = \sqrt{G_{SD}} h_{SD} x_1 + n_{SD} \ , \tag{1}$$

while the symbol received by the RN is:

$$y_{SR} = \sqrt{G_{SR}} h_{SR} x_1 + n_{SR} \ , \tag{2}$$

where the subscript SD denotes the SN-DN link and the subscript SR represents the SN-RN link. By contrast, the symbols received at the DN during the 2nd TS, which are sent by the RN, may be expressed as:

$$y_{RD} = \sqrt{G_{RD}} h_{RD} x_2 + n_{RD} \ , \tag{3}$$

where the subscript RD represents the RN-DN link. Additionally, the notations h_{SD}, h_{SR} and h_{RD} denote the complex-valued coefficients of the uncorrelated Rayleigh fading for the different links, while n_{SD}, n_{SR} and n_{SR} denote the Additive White Gaussian Noise (AWGN) having a variance of $N_0/2$ per dimension. Moreover, the terms G_{SD}, G_{SR} and G_{SR} represent the reduced-distance-related-pathloss-reduction for each link, which we also refer to as the path-gain. We consider an inverse-second-power law based free-space path-loss model [8] and naturally, the path-gain G_{SD} of the SD link is assumed to be unity. The position of the RN in our simulations is assumed to be right in the middle between the SN and DN. Therefore the path-gain of the SR link is:

$$G_{SR} = \left(\frac{d_{SD}}{d_{SR}} \right)^2 = 4 \ , \tag{4}$$

and similarly, the path-gain of the RD link is:

$$G_{RD} = \left(\frac{d_{SD}}{d_{RD}} \right)^2 = 4 \ . \tag{5}$$

The HM scheme and our communication protocol will be discussed in the following two sections.

III. Hierarchical Modulation

The general hierarchical constellation strategy was detailed in [4]. In contrast to the conventional HM scheme, the HM scheme used in our communication protocol has the following two main differences:

1) A new bit-to-symbol mapping method is defined, where the signal constellations is optimized according to the position of the RN.
2) The classic Set-Partitioning (SP) technique is employed in our TTCHM scheme and the symbol-based MAP algorithm is used for guaranteeing a minimum Symbol Error Ratio (SER).

However, the SP scheme would assign the parity bit to the least protected constellation-position, which would lead to a high BER for the parity bit. Fortunately, we will demonstrate that this does not jeopardize the overall BER of the information bits.

Fig. 2 shows our HM mapping scheme. Similar to the conventional HM scheme, we partition the coded symbols into different layers and map two data bits to each layer. The most important two bits represent the base layer. Their constellation points are defined by the set S_{4QAM}, which are represented by the four shaded circles in Fig. 2. Based on the above base layer, the twin-layer HM 16QAM symbols are generated using a parameter δ_1:

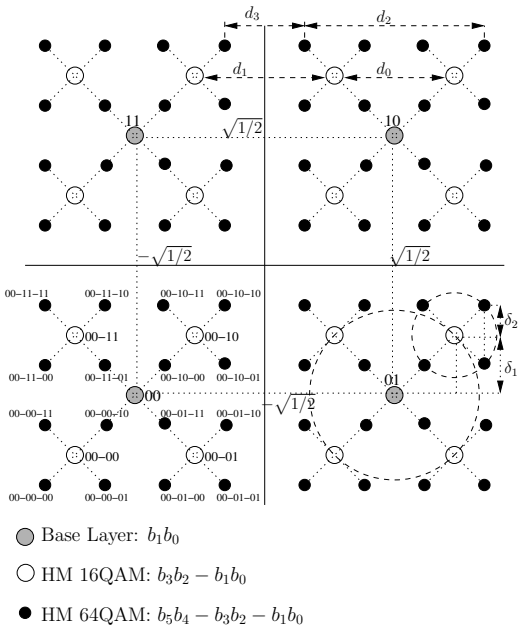

Fig. 2. The constellation map of the HM scheme.

$$S_{HM-16QAM} = \alpha \left[S_{4QAM} \pm \sqrt{2}\delta_1 e^{\pm \frac{\pi}{4} j} \right] \ , \tag{6}$$

where $\alpha = 1/\sqrt{1+2\delta_1^2}$ is the normalization parameter, which maintains the average symbol power of the $S_{HM-16QAM}$ constellation at unity. Furthermore, we define a HM parameter R_1, which equals to d_1/d_0 relying on the distances d_0 and d_1 seen in Fig. 2. The value of δ_1 (also seen in Fig. 2) depends on this R_1. When we change the value of R_1, the positions of the constellation points in the HM-16QAM would be changed. Here we have $\delta_1 = d_0/2$ and $d_0 + d_1 = \sqrt{2}$. The relationship between δ_1 and R_1 can be expressed as:

$$\delta_1 = \frac{d_0}{\sqrt{2}\sqrt{2}} = \frac{d_0}{\sqrt{2}\left(d_0 + d_1\right)} = \frac{1}{\sqrt{2}\left(1 + R_1\right)} \ . \tag{7}$$

It can also be observed that:

$$R_{1\max} = \frac{d_{1\max}}{d_{0\min}} = \frac{\sqrt{2}}{0} \Rightarrow \infty \ , \tag{8}$$

$$R_{1\min} = \frac{d_{1\min}}{d_{0\max}} = \frac{0}{\sqrt{2}} \Rightarrow 0 \ , \tag{9}$$

where, we have $0 < R_1 < \infty$.

Furthermore, the HM 64QAM constellations may be generated by adding a third layer to the twin-layer HM 16QAM signals upon introducing the HM parameter δ_2, which can be formulated as:

$$S_{HM-64QAM} = \beta \left[S_{4QAM} \pm \sqrt{2}\delta_1 e^{\pm \frac{\pi}{4} j} \pm \sqrt{2}\delta_2 e^{\pm \frac{\pi}{4} j} \right] \ , \tag{10}$$

where, δ_2 depends on the ratio of d_3/d_2, as shown in Fig. 2. We define $R_2 = d_3/d_2$ and the normalization parameter in Eq. (10) is given by $\beta = 1/\sqrt{1+2\delta_1^2+2\delta_2^2}$. It can be observed in Fig. 2

that we have $\delta_2 = \dfrac{(d_1 - d_3)}{2}$, which can be further written as:

$$\delta_2 = \frac{d_0\,(R_1 - R_2)}{2\,(1 + R_2)} = \frac{R_1 - R_2}{\sqrt{2}\,(1 + R_1)\,(1 + R_2)} \ . \quad (11)$$

Note that R_2 is directly restricted by R_1 as follows:

$$R_{2\max} = \frac{d_{3\max}}{d_{2\min}} = \frac{d_1}{d_0} \Rightarrow R_1 \ . \quad (12)$$

If $R_1 > 1$, then $\max(\delta_2) \to d_0/2$ and we have:

$$R_{2\min} = \frac{d_{3\min}}{d_{2\max}} = \frac{d_1 - d_0}{2d_0} \Rightarrow \frac{1}{2}(R_1 - 1) \ . \quad (13)$$

By contrast, if $R_1 < 1$, then we have $\max(\delta_2) \to d_3/2$ and hence:

$$R_{2\min} = \frac{d_{3\min}}{d_{2\max}} = \frac{0}{d_0 + d_3} \Rightarrow 0 \ . \quad (14)$$

In a nutshell, when generating a HM 64QAM symbol, the relationship between R_1 and R_2 can be expressed as:

$$\begin{cases} 0 < R_2 < R_1 & \text{if } \ R_1 < 1 \\ \dfrac{1}{2}(R_1 - 1) < R_2 < R_1 & \text{if } \ R_1 > 1 \ . \end{cases} \quad (15)$$

In our simulations, the HM mapping is controlled by the ratio of R_1 and R_2, which may be used for optimizing the performance of the system.

IV. Communication Protocol

Fig. 3 depicts the schematic of our communication scheme, where the twin-layer HM 16QAM is shown in Fig. 3(a), while the three-layer HM 64QAM is presented in Fig. 3(b). We mark the bits in the codeword of the HM 16QAM symbol as $b_3b_2 - b_1b_0$, where b_3b_2 occupy the base layer, which are also related to L_1, and b_1b_0 belong to the second layer L_2. By contrast, as shown in Fig. 2, the bits in the HM 64QAM symbol are grouped as $b_5b_4 - b_3b_2 - b_1b_0$, where the base layer L_1 contains b_5b_4, the second layer L_2 includes b_3b_2, while b_1b_0 are in the third layer L_3.

A. TTCHM-16QAM System

When the SN generates HM 16QAM frames, the HM scheme divides the 16QAM symbol into two layers, namely L_1 (b_3b_2) and L_2 (b_1b_0). As seen in Fig. 2, the two information bits in L_1 decide, which particular quadrant the transmitted symbol comes from and the two bits contained in L_2 illustrate the exact location of the transmitted symbol in each quadrant. The system's schematic is shown in Fig. 3(a), where the DN demaps x_1 as a 4QAM symbol for recovering the two-bit information contained in L_1 during the first TS. The probability of detecting L_1, when y_{SD} was received may be expressed as:

$$P(L_1^{(i)}|y_{SD}) = \frac{1}{\sqrt{\pi N_0}} \exp\left(-\frac{|y_{SD} - \sqrt{G_{SD}}h_{SD}S_{4QAM}^{(i)}|^2}{N_0}\right)$$
$$i \in \{0, 1, 2, 3\} \ . \quad (16)$$

However, the RN is capable of decoding the entire frame $\{x_1\}$ from the SN for detecting $L_1(b_3b_2)$ and $L_2(b_1b_0)$. Then, only the bit-pair $L_2(b_1b_0)$ is mapped to the general 4QAM symbols for transmission to the DN within the frame $\{x_2\}$. During a symbol period in the second TS, the DN will demap x_2 from the RN by computing the probability of receiving L_2, when y_{RD} was received:

$$P(L_2^{(j)}|y_{RD}) = \frac{1}{\sqrt{\pi N_0}} \exp\left(-\frac{|y_{RD} - \sqrt{G_{RD}}h_{RD}x_2^{(j)}|^2}{N_0}\right)$$
$$j \in \{0, 1, 2, 3\} \ . \quad (17)$$

Finally, the probability of the HM 16QAM symbol x_1 can be computed at the DN as:

$$P(L_1^{(i)}, L_2^{(j)}|x_1) = P(L_1^{(i)}|y_{SD}) \cdot P(L_2^{(j)}|y_{RD})$$
$$i, j \in \{0, 1, 2, 3\} \ . \quad (18)$$

Note that the DN would demap the signals x_1 and x_2 as two 4QAM symbols, but the number of modulation levels in the TTCHM decoding block of Fig. 3(a) is 16. Explicitly, we employ a rate-3/4 convolutional code as the constituent code of the Turbo Trellis-Coded Modulation (TTCM) [9]. The constraint length was chosen to be $k = 6$ and the generator polynomials (octal format) are $\mathbf{H}(\mathbf{D}) = [11\ \ 02\ \ 04\ \ 10]$. In our forthcoming investigations, we will adapt the parameter R_1 for optimizing the performance of the system. The related simulation results will be discussed in Section V.

B. TTCHM-64QAM System

When the SN generates HM 64QAM signal frames, there would be three layers in each HM symbol, namely L_1 (b_5b_4), L_2 (b_3b_2) and L_3 (b_1b_0). We employ a single RN in our cooperative communication system and we also divide the HM 64QAM symbol into two layers, namely L_H and L_L. The layer L_H is identical to the layer L_1 of the HM 16QAM scheme, but layer L_L contains both L_2 and L_3. In this way, both L_H and L_L would assume similar roles as L_1 and L_2 in HM 16QAM. As shown in Fig. 3(b), the DN would demap x_1 as a 4QAM symbol and the probability of receiving L_H conditioned on the reception of y_{SD} may be calculated as:

$$P(L_H^{(m)}|y_{SD}) = \frac{1}{\sqrt{\pi N_0}} \exp\left(-\frac{|y_{SD} - \sqrt{G_{SD}}h_{SD}S_{4QAM}^{(m)}|^2}{N_0}\right)$$
$$m \in \{0, 1, 2, 3\} \ . \quad (19)$$

Then, x_1 would be decoded by the RN for receiving the six data bits $b_5b_4b_3b_2b_1b_0$. However, only $b_3b_2b_1b_0$ of each 6-bit symbol would be mapped to a general 4-bit 16QAM symbol for transmission to the DN in form of the symbol x_2 during the second TS. Based on the symbol x_2, the probability of receiving L_L may be expressed at the DN as:

$$P(L_L^{(n)}|y_{RD}) = \frac{1}{\sqrt{\pi N_0}} \exp\left(-\frac{|y_{RD} - \sqrt{G_{RD}}h_{RD}x_2^{(n)}|^2}{N_0}\right)$$
$$n \in \{0, 1, \ldots, 15\} \ , \quad (20)$$

The symbol probability of the HM 64QAM symbol may be generated by combining the probabilities of L_H and L_L as:

$$P(L_H^{(m)}, L_L^{(n)}|x_1) = P(L_H^{(m)}|y_{SD}) \cdot P(L_L^{(n)}|y_{RD})$$
$$m \in \{0, 1, 2, 3\}, n \in \{0, 1, \ldots, 15\} \ . \quad (21)$$

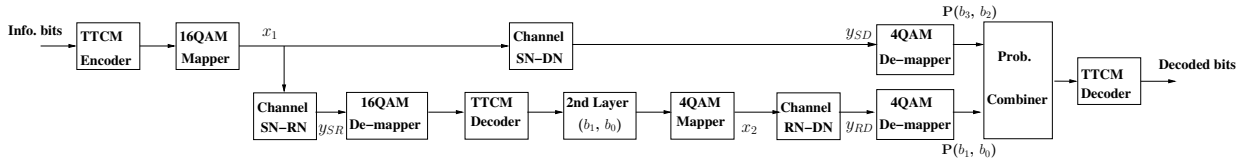

(a) Two-Layer HM 16QAM

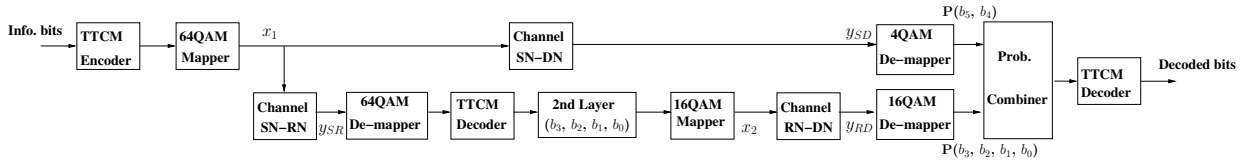

(b) Three-Layer HM 64QAM

Fig. 3. The block diagram of the cooperative communication system.

Note that when the number of modulation levels of the HM scheme is 64, the six data bits in each codeword are still divided into two layers, namely L_H and L_L, where there are two bits in layer L_H, while the layer L_L contains four bits. In this situation, there are two different symbol-to-bit demapper blocks at the DN, the first one is a 4QAM demapper, which is activated during the first TS, while the second one is a 16QAM demapper, which is activated during the second TS at the DN. The rate 5/6 encoder of the 64QAM-based TTCM scheme [9] is used in our TTCHM scheme. The constraint length was chosen to be $k = 20$ and the generator polynomials (octal format) are $\mathbf{H}(\mathbf{D}) = [41\ \ 02\ \ 04\ \ 10\ \ 20\ \ 40]$. The parameters R_1 and R_2 will be jointly adapted for optimizing the performance of the entire system.

V. Simulation Results

In this section, we provide our simulation results for characterizing the proposed TTCHM assisted cooperative communication systems. Again, our channel model is the uncorrelated Rayleigh fading channel and the receiver has the perfect CSI. Firstly, the performance of the TTCHM-16QAM scheme is presented and the related simulation results are displayed in Fig. 4 to Fig. 6.

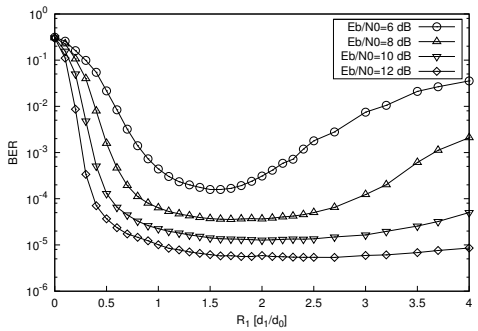

Fig. 4. The BER versus R_1 performance of the TTCHM-16QAM aided single relay cooperative communications over uncorrelated Rayleigh fading channels. The performance curves are based on different HM ratio R_1 when given E_b/N_0 $[dB] = \{6, 8, 10, 12\}$. A block length of 1200 is employed and the number of turbo iterations is fixed to four.

Fig. 4 characterizes the relationship between the BER performance of the TTCHM-16QAM and the ratio R_1. We considered the BER performance of the system to be a function of the ratio R_1, while considering four different average bit power to noise ratio of E_b/N_0. It can be observed from Fig. 4 that when $E_b/N_0 = 6$ dB, the best BER performance is attained at $R_1 = 1.6$, while at $R_1 = 1.7$ for $E_b/N_0 = 8$ dB, $R_1 = 2.0$ for $E_b/N_0 = 10$ dB and $R_1 = 2.5$ for $E_b/N_0 = 12$ dB.

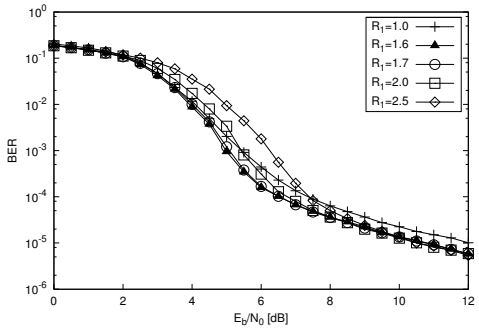

Fig. 5. The BER versus E_b/N_0 performance of the TTCHM-16QAM aided single relay cooperative communications over uncorrelated Rayleigh fading channels. The performance curves are based on different HM ratio R_1 when given $R_1 = \{1.0, 1.6, 1.7, 2.0, 2.5\}$. A block length of 1200 is employed and the number of turbo iterations is fixed to four.

Fig. 5 compares the BER performance of our TTCHM-16QAM schemes for different R_1 values. Four of the five R_1 values are based on the simulation results shown in Fig. 4, while $R_1 = 1$ is also included, which represents the general square 16QAM mapping. It was found that the performance of our TTCHM-16QAM aided cooperative system is optimized at $R_1 = 1.6$. As seen in Fig. 5, the performance of the entire system associated with the ratio of $R_1 = 1.6$ is about 1.5 dB better than that of the general square mapping HM scheme at BER=10^{-5}.

Furthermore, we compared the BER performance of every single bit in the codeword symbol of the optimized TTCHM-16QAM scheme in Fig. 6. It can be stated that the BER of b_3 is similar to the overall BER performance of the three information bits and it is about 1.5 dB

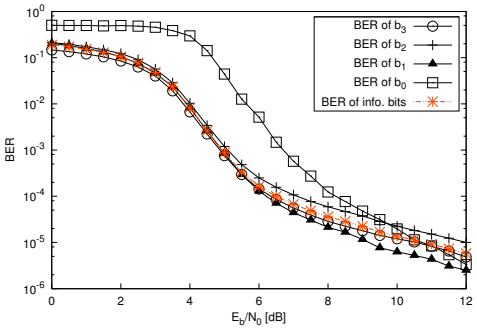

Fig. 6. The BER versus E_b/N_0 performance of the TTCHM-16QAM aided single relay cooperative communications over uncorrelated Rayleigh fading channels. The performance curves are based on HM ratio $R_1 = 1.6$, and each single bit in the codeword symbol namely b_3, b_2, b_1 and b_0 are separated. While, b_3, b_2 and b_1 are information bits, b_0 is the parity bit. A block length of 1200 is employed and the number of turbo iterations is fixed to four.

worse than that of b_1, but about 1.2 dB better than that of b_2, as recorded at BER=10^{-6}. Note that the BER performance of the three information bits is within a ± 1.5 dB range of the overall BER performance of the three information bits at a BER of 10^{-6}. However, as mentioned in Section III, when the signal power is low, the BER performance of the parity bit b_0 is at least 2 dB worse than that of the information bits. This is mainly because the parity bit in the SP scheme has the lowest minimum Euclidean distance. Fortunately, the performance of the parity bit does not degrade the performance of the three information bits.

Next, we investigated the attainable performance of our TTCHM-64QAM scheme. The related simulation results are displayed in Fig. 7 to Fig. 9. Since the TTCHM-64QAM scheme is controlled by the pair of HM ratios R_1 and R_2, we have used two typical values of R_1, namely 1.0 and 1.6. When $R_1 = 1$, the HM 16QAM becomes the original square mapping and $R_1 = 1.6$ represents the best configuration of the TTCHM-16QAM scheme in cooperative communications according to our results in Fig. 5. The comparisons are carried out separately based on these two R_1 values.

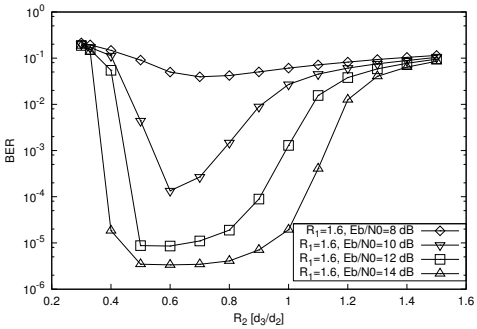

Fig. 7. The BER versus R_2 performance of the TTCHM-64QAM aided single relay cooperative communications over uncorrelated Rayleigh fading channels. The performance curves are based on different HM ratio R_2 when given $R_1 = 1.6$ and E_b/N_0 $[dB] = \{8, 10, 12, 14\}$. A block length of 1200 is employed and the number of turbo iterations is fixed to four.

It can be observed in Fig. 7 and Fig. 8 that when choosing $R_1 = 1.6$, the best performance is achieved for $R_2 = 0.6$. By contrast, the system attained its best performance for $R_2 = 0.33$ at $R_1 = 1$. Note that when the HM 64QAM ratio pair is $[R_1 = 1.0, R_2 = 0.33]$, the constellations will be turned into the original square 64QAM mapping. In Fig. 9, we picked the HM ratio parameter pairs of [1.0, 0.33], [1.0, 0.4], [1.6, 0.33] and [1.6, 0.6] to perform a BER versus E_b/N_0 comparison. The results show that when the E_b/N_0 value is between 8 dB and 10 dB, the system associated with the ratio parameter pair of [1.0, 0.33] performs about 1 dB better than that with the ratio pair [1.6, 0.6]. However, when E_b/N_0 is higher than 11 dB, the system relying on the ratio pair of [1.6, 0.6] turns out to be better. More explicitly, it is about 0.5 dB better than that associated with the ratio pair of [1.0, 0.33] at BER=10^{-5}.

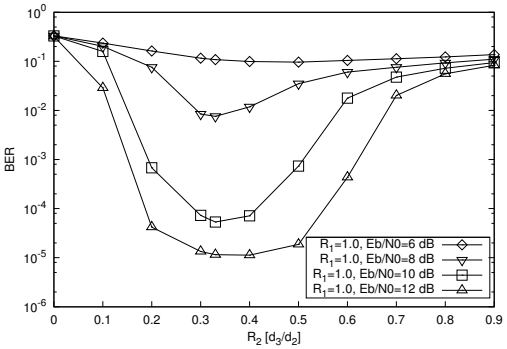

Fig. 8. The BER versus R_2 performance of the TTCHM-64QAM aided single relay cooperative communications over uncorrelated Rayleigh fading channels. The performance curves are based on different HM ratio R_2 when given $R_1 = 1.0$ and E_b/N_0 $[dB] = \{8, 10, 12, 14\}$. A block length of 1200 is employed and the number of turbo iterations is fixed to four.

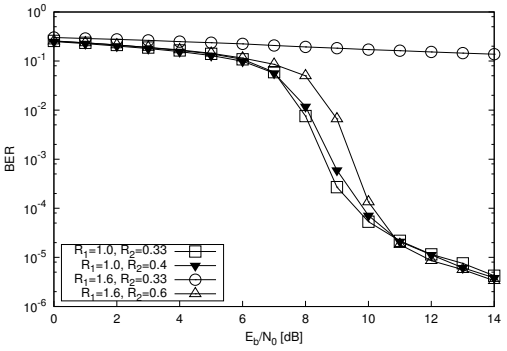

Fig. 9. The BER versus E_b/N_0 performance of the TTCHM-64QAM aided single relay cooperative communications over uncorrelated Rayleigh fading channels. The performance curves are based on different HM ratio pair $[R_1, R_2]$ when given $[R_1, R_2] = \{[1.0, 0.33], [1.0, 0.4], [1.6, 0.33], [1.6, 0.6]\}$. A block length of 1200 is employed and the number of turbo iterations is fixed to four.

Similar to the investigations reported in Fig. 6, the BER recorded for each of the six coded bits in our TTCHM-64QAM scheme are shown in Fig. 10. It can be stated that the BER performance of the two bits contained in the first layer ($b_5 b_4$) is better than the

average BER performance of the other information bits ($b_3b_4b_5b_6$). On the other hand, there are only moderate differences among the performances of the three information bits contained in the second layer. Furthermore, they are all close to the average BER performance of the five information bits. At a BER of 10^{-5}, the required E_b/N_0 of the first bit (b_5) in the codeword is about 11.5 dB, which is about 1.5 dB better than that of the average BER of the five information bits. The E_b/N_0 differences among the other four information bits are within a ± 1 dB range. Although the BER performance of the parity bit b_0 is not as good as that of the others, this does not degrade the overall performance of the information bit. The simulation results of Fig. 10 show that the BER of each information bit in the TTCHM-64QAM scheme is similar.

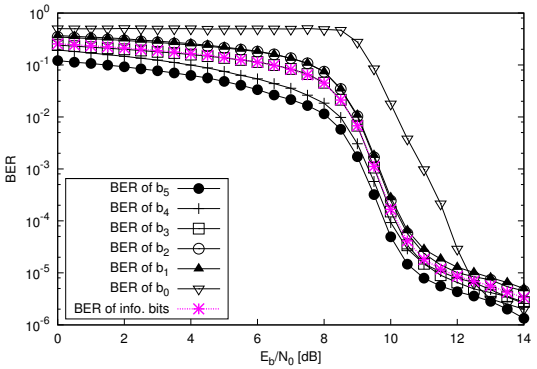

Fig. 10. The BER versus E_b/N_0 performance of the TTCHM-64QAM aided single relay cooperative communications over uncorrelated Rayleigh fading channels. The performance curves are based on HM ratio pair [$R_1 = 1.6$, $R_2 = 0.6$], and each single bit in the codeword symbol namely b_5, b_4, b_3, b_2, b_1 and b_0 are separated. While, b_5, b_4, b_3, b_2 and b_1 are information bits, b_0 is the parity bit. A block length of 1200 is employed and the number of turbo iterations is fixed to four.

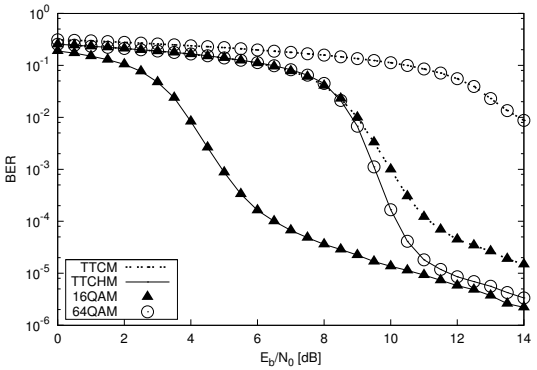

Fig. 11. The BER versus E_b/N_0 curves of the TTCHM aided cooperative communications against the non-cooperative communications. The HM 16QAM scheme is using a HM ratio $R_1 = 1.6$, and the HM ratio pair for the HM 64QAM scheme is [1.6, 0.6]. A block length of 1200 is employed and the number of turbo iterations is fixed to four.

When compared to the non-cooperative single-input-single-output (SISO) TTCM schemes, our solution attains a remarkable improvement. The related simulation results are shown in Fig. 11. The cooperative TTCHM-16QAM aided system performs about 4 dB better than the non-cooperative TTCM-16QAM system at a BER of 10^{-5}. By comparison, the original non-cooperative system relying on the TTCM-64QAM scheme failed to reach a BER of 10^{-3} for E_b/N_0 values below 24 dB. By contrast, our TTCHM-64QAM cooperative communication system exhibited a BER of 10^{-5} at $E_b/N_0 = 12$ dB, which is about 2.5 dB better than that of the non-cooperative TTCM-16QAM schemes.

VI. Conclusions

In this paper, a TTCHM aided cooperative communication scheme was proposed. We amalgamated cooperative communication, TTCM channel coding and a HM scheme for attaining further performance gains. Our simulation results have demonstrated that the BER performance of the entire system was increased without reducing the coding rate or adding extra transmission power. However, the ratio R of the HM scheme depends on the position of the RN, where the optimum ratio pairs found for our TTCHM scheme have to be updated using a position-based look-up table, when the RN is not located in the mid-point between the SN and DN. Our future work aims for finding the globally optimum ratio pair.

References

[1] S. Wang, S. Kwon, B. K. Yi, "On enhancing hierarchical modulation," *IEEE International Symposium, Broadband Multimedia Syatem and Broadcasting*, vol. , pp. 1–6, Jun 2008.

[2] R. Y. Kim, Y-Y. Kim, "Symbol-level random network coded cooperation with hierarchical modulation in relay communication," *IEEE Transactions on, Consumer Electronics*, vol. 55, pp. 1280–1285, Oct 2009.

[3] L. Hanzo, J. Blogh, S. Ni, *3G, HSPA and FDD versus TDD networking:smart antennas and adaptive modulation*. New York: Wiley-IEEE, 2nd ed., 2008.

[4] M. J. Hossain, M. S. Alouini, V. K. Bhargava, "Rate adaptive hierarchical modulation-assisted two-user opportunistic scheduling," *IEEE Transactions on, Wireless Communications*, vol. 6, pp. 1536–1276, Aug 2007.

[5] M. J. Hossain, P. K. Vitthaladevuni, M. S. Alouini, V. K. Bhargava, A. J. Goldsmith, "Adaptive hierarchical modulation for simultaneous voice and multiclass data transmission over fading channels," *IEEE Transactions on, Vehicular Technology*, vol. 55, pp. 1181–1194, Jul 2006.

[6] C. Hausl and J. Hagenauer, "Relay communication with hierarchical modulation," *IEEE Communications Letters*, vol. 11, pp. 64–66, Jan 2007.

[7] Z. Y. Li, M. G. Peng and W. B. Wang, "Hierarchical modulated channel and network coding scheme in the multiple-access relay system," *IEEE 13th International Conference on Communication Technology (ICCT)*, vol. , pp. 984–988, Sep 2011.

[8] H. Ochiai, P. Mitran, V. Tarokh, "Design and analysis of collaborative diversity protocols for wireless sensor networks," *Vehicular Technology Coference, VTC2004-Fall, IEEE 60th* , vol. 7, pp. 4645–4649, sep 2004.

[9] P. Robertson and T. Worz, "Band-efficient turbo trellis-coded modulation using punctured component codes," *IEEE Journal on Selected Areas in Communications*, vol. 16, pp. 206–218, Feb 1998.